ELSEVIER

Journal of Chromatography A, 734 (1996) 145–154

JOURNAL OF CHROMATOGRAPHY A

Simulation of the combined continuous and preparative gas–liquid chromatographic separation of three close-boiling components

Kyung Ho Row

Department of Chemical Engineering, Inha University, 253 Yonghyun-Dong, Nam-Ku, Inchon, South Korea

Abstract

A combined continuous and preparative gas–liquid chromatographic system was considered for separating continuously three close-boiling components, diethyl ether, dimethoxymethane and dichloromethane. Their concentration profiles were simulated by a mathematical model that assumed the uniform distribution of stationary liquid phase and linearity of the equilibrium isotherm. The operational principles of the system are that the least absorbed component of the three components can be obtained purely before the elution of the more absorbed components if the mixture is continuously injected into one of the two sections (partition section) and at the same time, in the other section (desorption section), the three components remaining in the column can be separated by adjusting the experimental conditions and the column configuration. If the operations in the two sections are simultaneously finished within the switching time, continuous separations of the three components are feasible. Effects of various operating conditions on the resolution were investigated. The results of the simulations indicated that the resolution was greatly affected by the additional column length in the desorption section and the switching time could be determined by the desorbent velocity.

Keywords: Preparative chromatography; Continuous beds; Simulation techniques; Diethyl ether; Dimethoxymethane; Dichloromethane

1. Introduction

One of the advantages of gas chromatographic separation over simple distillation is that separation can be achieved even in cases of small differences in boiling points [1]. In this work, three materials with closely similar boiling points, dichloromethane, diethyl ether and dimethoxymethane, were studied for their combined continuous and preparative gas–liquid chromatographic separation by the prediction of the calculated elution profiles.

With the first introduction of chromatography, it was recognized this technology could be used for quantitative separations on an industrial scale [2]. Many attempts have been made to scale up laboratory-sized chromatographic units to treat greater amounts of substances and to make the system a continuous operation [3,4]. By the early 1960s, continuous countercurrent moving-bed separators were used to separate binary components in laboratory-scale equipment [5,6], and the characteristics of this system were well documented in [7]. Later, this system was examined

0021-9673/96/$15.00
SSDI 0021-9673(95)00984-1

further with an ideal mathematical model which predicted the concentration profile around the feed point of the unit [8].

The UOP (Universal Oil Products) process is widely acknowledged as one of the earliest simulated moving bed (SMB) systems [9]. Two mathematical models of the moving bed adsorber, an intermittent moving bed and a continuous moving bed type, were presented by Hashimoto and co-workers [10,11] for calculating the concentration profiles of glucose and fructose. For the semi-continuous counter-current refiner (SCCR), a mathematical model based on the theoretical plate concept was used to simulate its performance [12]. Ching and Ruthven [13,14] proposed a theoretical model for simulated counter-current operation as an equivalent counter-current cascade of theoretical equilibrium stage under steady-state conditions and obtained the analytical concentration profile. More recently, the design and performance for the optimum operating conditions of SMB units have been considered by numerous workers [15–17].

In a related process, Wankat [18,19] used a local equilibrium model to analyse the characteristics of a moving feed-point system, while the plate model was used to predict the concentration profiles for the same system [20].

For a combined continuous and preparative chromatographic system, mathematical models have been developed and used to compare the experimental data with the calculated values in the binary system of diethyl ether and dichloromethane [21,22]. The purpose of this work was to investigate the usefulness of this system for the separation of the three close-boiling components and the effects of operating conditions on the column efficiency expressed as the number of theoretical plates in the partition section and the resolution of the components in the desorption section by the prediction of concentration profiles.

2. Operational principles of the system

When a mixture of diethyl ether (DEE), dimethoxymethane (DMM) and dichloromethane (DCM) (all from Kanto Chemical, Tokyo, Japan) is continuously injected into the inlet of a chromatographic column, DEE is eluted first owing to the solubility difference with the stationary liquid phase (SLP) of dinonyl phthalate (Tokyo Kasei, Tokyo, Japan), and subsequently DCM followed by DMM leave from the column [21,22]. The feed mixture is continuously injected until only the least absorbed component (DEE) leaves the column in the partition section, and the unseparated components in the partition section can be separated with adjustments to the column length and desorbent velocity in the desorption section. The experimental system is composed of twelve segmented columns and 60 solenoid valves controlled by a programmable controller (see Fig. 1). The partition section is assumed to consist of four columns and the desorption section of eight columns. During the first switching time, the feed is continuously injected into column 1, pure DEE is obtained at the outlet of column 4. Within the second switching time, the position of feed injection is moved to the inlet of column 9. At the same time, columns 1–8 constitute the desorption section, and a mixture of three components is separated at the outlet of column 8.

Separation of the components is continuously achieved if the operations in the two sections are terminated within the switching time, and the feed mixture is systematically injected into the following columns with a circular form. In the partition section, only DEE is obtained in a pure state, and in the desorption sections with additional columns, the remaining DEE, DMM and DCM in the columns. The following mathematical models were set up and used to predict the feasibility of this chromatographic system for ternary components with close boiling points and the performance of the system.

3. Mathematical models

The basic equations for this system are well known [21–24]. The assumptions for establishing the equations governing the processes are a uniformly distributed SLP on the surface of the

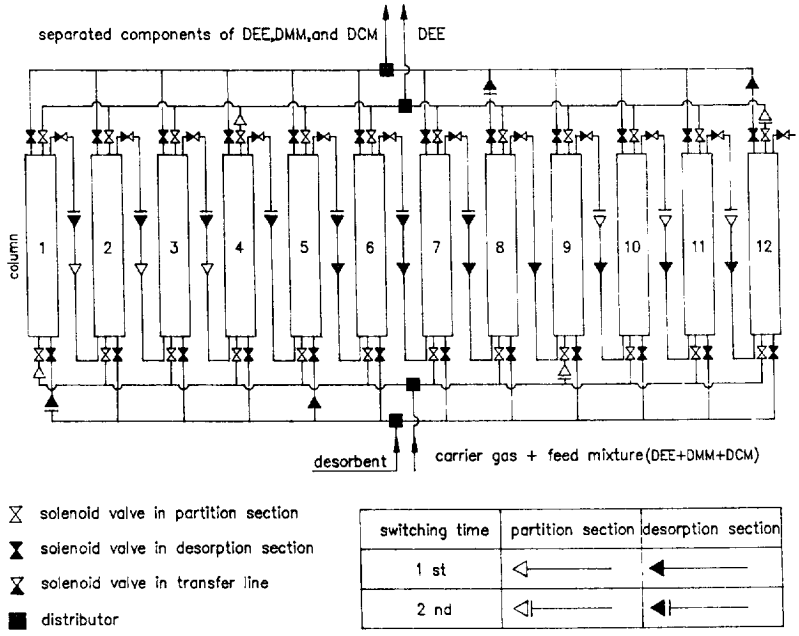

Fig. 1. Schematic diagram of combined continuous and preparative chromatographic beds.

inert solid particle, a linear partition isotherm, negligible sorption and pressure drop effects and spherical solid particles. The following Laplace transformed equation can be used to predict the concentration profile of the least absorbed component in the partition section for an injection time t_0:

$$C(s) = \frac{1 - e^{-st_0}}{s} \times \exp\left(\frac{L}{2}\left\{\frac{u_0}{E} - \left[\left(\frac{u_0}{E}\right)^2 + 4\lambda\right]^{1/2}\right\}\right) \quad (1)$$

at the bed exist, $Z = L$, where

$$\lambda = \frac{\epsilon}{E}\left\{s + \frac{3(1-\epsilon)}{r_p \epsilon} k_f \left[1 - \frac{\sinh(\lambda_2 r_p)}{r_p}\lambda_1\right]\right\} \quad (2)$$

$$\lambda_1 = \frac{r_p k_f}{D_e \lambda_2 \cosh(\lambda_2 r_p) + \left(k_f - \frac{D_e}{r_p}\right)\sinh(\lambda_2 r_p)} \quad (3)$$

$$\lambda_2 = \left\{\frac{1}{D_e}\left[(\epsilon_p s + A_p k_g) - \frac{A_p k_g^2 \cosh(\lambda_3)}{D_e K\left(\frac{s}{D_1}\right)^{1/2}\lambda_e + D_e k_g \cosh(\lambda_3)}\right]\right\}^{1/2} \quad (4)$$

$$\lambda_3 = \delta\left(\frac{s}{D_1}\right)^{1/2} \quad (5)$$

In the desorption section, the components are assumed to be partitioned initially with the inlet concentration of the feed, c_0. The governing equations are the same as those in the partition section. However, some of the initial and boundary conditions are different from those in the partition section. The initial conditions and the boundary conditions in the desorption section are changed as follows:

$$c = q = c_0 \quad (\text{for } t = 0, z > 0) \quad (6)$$

$$n = Kc_0 \quad (\text{for } t = 0, z > 0) \quad (7)$$

$$c = 0 \quad (\text{for } t > 0, z = 0) \quad (8)$$

Under these conditions, the solution in the Laplace domain with the additional column length (L') is

$$C(s) = \gamma\left[\exp\left(\frac{L}{2}\left\{\frac{u_0}{E} - \left[\left(\frac{u_0}{E}\right)^2 + 4\gamma_1\right]^{1/2}\right\}\right) - 1\right] \times \exp\left(\frac{L'}{2}\left\{\frac{u_0}{E} - \left[\left(\frac{u_0}{E}\right)^2 + 4\lambda\right]^{1/2}\right\}\right) \quad (9)$$

$$\gamma = \left\{-\frac{\epsilon_p c_0}{E} + \frac{3(1-\epsilon_p)}{r_p E} \cdot k_f\left[\frac{\gamma_2 \sinh(\sqrt{\gamma_4} r_p)}{r_p} + \frac{\gamma_5}{\gamma_4}\right]\right\}/\gamma_1 \quad (10)$$

$$\gamma_1 = -\frac{\epsilon s}{E} + \frac{3(1-\epsilon)}{r_p E} \cdot k_f\left[1 - \frac{\gamma_3 \sinh(\sqrt{\gamma_4} r_p)}{r_p}\right] \quad (11)$$

$$\gamma_2 = -\gamma_5 k_f/(\gamma_4\{D_e[\sqrt{\gamma_4} r_p \cosh(\sqrt{\gamma_4} r_p) - \sinh(\sqrt{\gamma_4} r_p)]/r_p^2 + k_f \sinh(\sqrt{\gamma_4} r_p)/r_p\}) \quad (12)$$

$$\gamma_3 = \frac{-\gamma_4}{\gamma_5 \gamma_2} \quad (13)$$

$$\gamma_4 = \frac{1}{D_e}(\epsilon_p s + A_p k_g) - \frac{A_p k_g^2 \cosh\left[\left(\frac{s}{D_1/2}\right)^{1/2}\delta\right]}{D_e K\left\{\sqrt{D_1 s}\sinh\left[\left(\frac{s}{D_1}\right)^{1/2}\delta\right] + k_g \cosh\left[\left(\frac{s}{D_1}\right)^{1/2}\delta\right]/K\right\}} \quad (14)$$

$$\gamma_5 = \frac{A_p k_g}{D_e K} \times \left\{\frac{Kc_0}{s} - \frac{\frac{k_g c_0}{s}\cosh\left[\left(\frac{s}{D_1}\right)^{1/2}\delta\right]}{\sqrt{D_1 s}\sinh\left[\left(\frac{s}{D_1}\right)^{1/2}\delta\right] + k_g \cosh\left[\left(\frac{s}{D_1}\right)^{1/2}\delta\right]/K}\right\} + \frac{c_0}{D_e} \quad (15)$$

The resulting Laplace transformed equations (Eqs. 1 and 9) should be converted into the real time domain to predict the elution profiles in the partition section and the desorption section, respectively. Using an HP Vectra PC (Model 486/66VL), the equations are inverted numerically with the curve-fitting procedure by Dang and Gibilaro [25]. The parameters used in the simulations are listed in Table 1. For each component, the axial dispersion coefficient, E, was estimated from the correlation $E = 0.707 D_M + r_p u_0^{1.539}$ and the effective diffusivity, D_e, was obtained by the analysis of frequency domain [22,23]. The diffusion coefficient in SLP, D_1, was calculated from the Wilke–Chang equation using the molar volume by the Tyn and Calus method for an SLP of dinonyl phthalate [22,23]. The dependence of interparticle mass transfer coefficient, k_f, on the superficial velocity of the eluent and particle size was expressed by the following semi-empirical correlation [26]:

$$k_f = \frac{D_M}{2r_p}(2 + 1.45 Re^{0.50} Sc^{0.33}) \quad (16)$$

For the intraparticle mass transfer coefficient, k_g, the following correlation formula proposed by Ergun [27] was used with the assumption that it was not affected by the superficial velocity of the eluent:

$$k_g = 12.5\left[\frac{D_M(1-\epsilon_p)}{r_p \epsilon_p}\right] \quad (17)$$

4. Results and discussion

When a mixture of DEE, DMM and DCM is continuously injected, the concentration profiles in partition section are as shown in Fig. 2. The curves in the partition section were calculated by numerical inversion of the Laplace transformed Eq. 1. In this case, the switching time is determined as 90 s just before the elution of DMM.

The effects of the operating conditions on the number of theoretical plates (N) in the partition section are given in Table 2. Under the assumption of a large theoretical number of plates [28], it is calculated by the following equation:

$$N = 2\pi(v_{1/2}/w)^2 \quad (18)$$

where $v_{1/2}$ and w are the retention volume corresponding to half-height and the intercept under the tangent at the point of inflection in units of volume, respectively. As the column temperature was increased, the total elution

Table 1
Parameters used in simulation work

Particle size (mesh)	60–80			45–60			20–30		
r_p (m)	0.0000996			0.000136			0.000314		
Liquid loading (%)	25	20	15	25	20	15	25	20	15
ϵ_p	0.62	0.66	0.69	0.62	0.66	0.69	0.50	0.54	0.57
Liquid loading (%)	25			20			15		
δ ($m \times 10^{-6}$)	0.1270			0.0955			0.0650		

35°C	DEE[a]	DMM[a]	DCM[a]
D_M (10^{-5} m^2/s)	0.93	1.00	1.08
D_c (10^{-9} m^2/s)	1.00	1.19	2.00
D_1 (10^{-10} m^2/s)	0.66	0.79	0.90
K	126.3	180.5	297.1

A_p (m^2/m^3)	1 300 000.0
ϵ	0.41

[a] 35°C

volume of the carrier gas necessary to exclude the component from the column was smaller, because the partition coefficient deceased exponentially with temperature [23]. In the partition section the column temperature has a direct effect on the switching time, that is, a higher column temperature resulted in a shorter switching time. Table 2 also shows that the number of theoretical plates was considerably affected by the change in the percentage liquid loading defined by the percentage ratio of the mass of SLP to that of uncoated solid packings. The elution time of a component was shorter at lower liquid loadings, so more feed mixtures cannot be separated because of the limited amount of SLP. However, higher liquid loadings increased the separation time. In such a case with a high temperature in the system, it is often detrimental to the capacity of a column, since the relative retention volumes between two components diminish with increase in temperature. Therefore, an optimum liquid loading might exist in a practical operation. As a large amount of feed is usually injected in a scaled-up chromatographic system, column packings with high liquid loadings were generally used. Fine particles sharpened the leading edge of the concentration profile in the partition section due to the in-

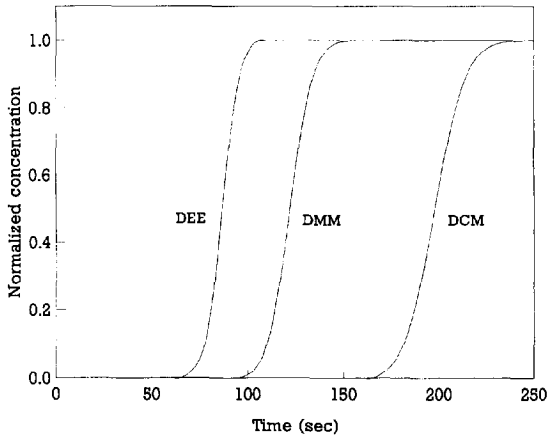

Fig. 2. Theoretical concentration profiles in partition section. $L = 1.0$ m, $u_0 = 0.15$ m/s, 35°C, 25% liquid loading, 45–60 mesh.

Table 2
Number of theoretical plates (N) in partition section

u_0 (m/s)	Column temperature (°C)	Liquid loading (%)	Particle size (mesh)	N		
				DEE	DMM	DCM
0.02	35	20	45–60	859	1103	1580
0.03	35	20	45–60	334	665	845
0.04	35	20	45–60	316	509	971
0.05	35	20	45–60	377	465	540
0.10	35	20	45–60	377	323	341
0.15	35	20	45–60	124	204	358
0.20	35	20	45–6 – 0	179	72	166
0.25	35	20	45–60	97	50	84
0.15	25	15	45–60	183	149	270
0.15	25	25	45–60	96	131	141
0.15	30	15	45–60	123	169	238
0.15	30	25	45–60	64	105	173
0.15	35	15	45–60	109	111	131
0.15	35	25	45–60	54	112	139
0.15	40	15	45–60	75	58	183
0.15	40	25	45–60	55	91	135
0.15	45	15	45–60	83	109	188
0.15	45	25	45–60	70	72	115
0.15	25	20	20–30	19	21	42
0.15	25	20	45–60	157	173	202
0.15	25	20	60–80	353	170	291
0.15	30	20	20–30	21	27	42
0.15	30	20	45–60	88	86	205
0.15	30	20	60–80	230	145	312
0.15	35	20	20–30	26	25	44
0.15	35	20	45–60	143	93	138
0.15	35	20	60–80	173	181	305
0.15	40	20	20–30	18	24	48
0.15	40	20	45–60	57	102	197
0.15	40	20	60–80	57	108	195
0.15	45	20	20–30	9	25	35
0.15	45	20	45–60	45	77	112
0.15	45	20	60–80	86	111	185

creased column efficiency. However, in a gas chromatographic column, a larger pressure drop caused by smaller particle sizes was not desirable, because the best column efficiency is obtained at a low inlet-to-outlet ratio of the pressure throughout the column. The majority of practical gas chromatographic systems are normally performed with the outlet at atmospheric pressure, so that the inlet pressure is adjusted to operate at the optimum flow-rate in the chromatographic column.

The concentration profiles of the three components in the desorption section are shown in Fig. 3. The curves in the desorption section were calculated by numerical inversion of the Laplace transformed Eq. 9. The effect of the desorbent velocity on the total elution time with additional columns in the desorption section is shown in Fig. 4. The desorbent velocity needs to be adjusted for the remaining components to be completely eluted from the desorption section within the switching time to achieve continuous opera-

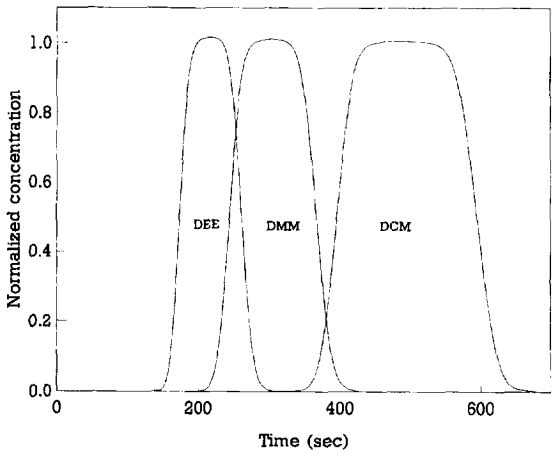

Fig. 3. Theoretical concentration profiles in desorption section. $L = 1.0$ m, $L' = 2.0$ m, $u_0 = 0.15$ m/s, 35°C, 25% liquid loading, 45–60 mesh.

tion. Under certain conditions in the partition section, the switching time can be determined as the duration from the start-up of injection to just before the elution of DMM.

The resolution is used to investigate the optimum operating conditions, and is defined by

$$R_{1,2} = 2(b_2 - b_1)/(a_2 + a_1) \quad (19)$$

where a_i and b_i are the peak width of component i cut by the two tangents in units of volume and the retention volume of component i from injection to peak maximum, respectively. With increase in the additional column length in the desorption section, the two resolutions of neighbouring components were gradually improved (Fig. 5). In analytical chromatography, the shape of a peak is sharp, whereas in a preparative system, the top is flattened, caused by the larger volume of feed mixture [29].

The effect of column temperature in the desorption section on the resolution is shown in Fig. 6. The components were eluted faster with higher temperature. In this system, the column temperature was to be kept uniform in the two sections. Because a higher temperature decreases the total elution time, the resolution may be worse owing to the rapid elution of the two components. For a 20% liquid loading, the optimum column temperature is about 41°C, which was slightly above the boiling points of DEE and DCM. The chromatographic separation is operated around the boiling points of the components to be separated [30].

A high percentage liquid loading increased the resolution (Fig. 7), but it also increased the total elution time. A smaller particle size improved the resolution (Fig. 8).

The separation of the three components in the desorption section was decisively affected by an

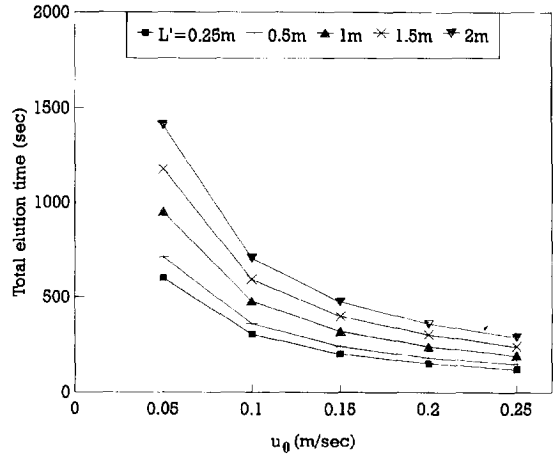

Fig. 4. Effect of desorbent velocity with additional column length on total elution time in desorption section. $L = 1.0$ m, 35°C, 20% liquid loading, 45–60 mesh.

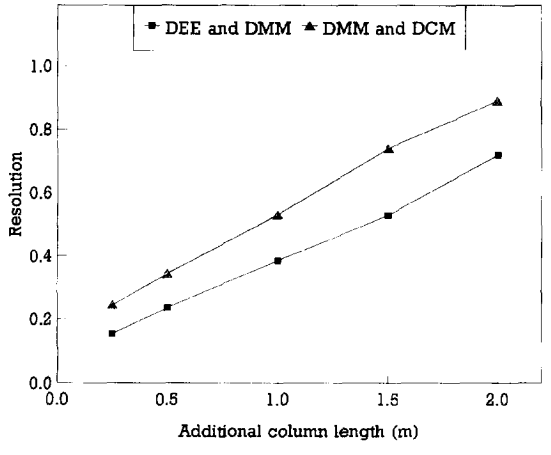

Fig. 5. Effect of additional column length on resolution in desorption section. $L = 1.0$ m. $u_0 = 0.15$ m/s, 35°C, 20% liquid loading, 45–60 mesh.

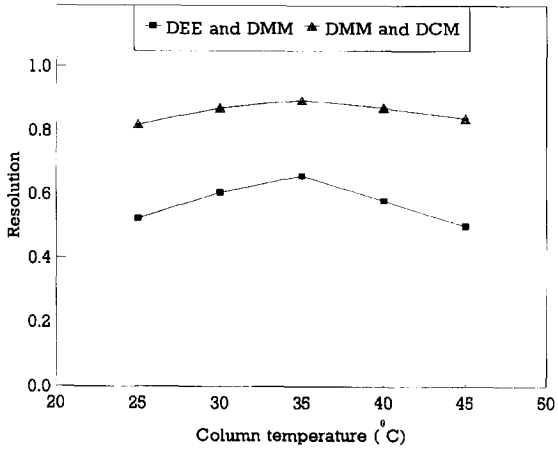

Fig. 6. Effect of column temperature on resolution in desorption section. $L = 1.0$ m, $L' = 2.0$ m, $u_0 = 0.15$ m/s, 20% liquid loading, 45–60 mesh.

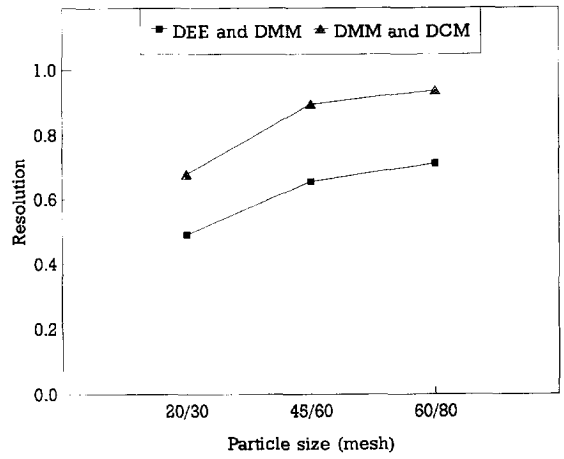

Fig. 8. Effect of particle size on resolution in desorption section. $L = 1.0$ m, $L' = 2.0$ m, $u_0 = 0.15$ m/s, 35°C, 20% liquid loading.

increase in the additional column length, more so than by particle size and percentage liquid loading. By adjusting the desorbent velocity, the remaining components in the desorption section should be separated within the switching time to perform the operation of the system continuously. Therefore, a suitable selection of particle size and loading of SLP is necessary to meet the conditions of the switching time.

The uniqueness of this system was that several columns were added in series in the desorption section to separate the non-eluted components effectively, compared with other continuous chromatographic systems. In the binary system of DEE and DCM, the theoretical concentration profiles calculated by the same mathematical models were in relatively good agreement with the experimental data [21,22]. In the model equations, the assumptions were that the equilibrium isotherm was linear and no interaction between the components existed. When the feed concentration is increased, the phenomena in the column become more complex, and the information about the non-linear isotherm is needed for a better prediction. Moreover, the assumption that the velocity of carrier gas or desorbent remained constant throughout a column is thought not to be reasonable, because a higher pressure drop caused by a smaller particle size and a longer column length led to variations in the gas velocity, and the changes in solute concentration along the length of a column by absorption is necessarily accompanied by a change in the velocity. Although it was assumed in Eq. 6 that the components were uniformly partitioned in the desorption section with the feed concentration c_0, for the more absorbed components this was not exactly so, because during the previous switching time, the component was not withdrawn from the partition

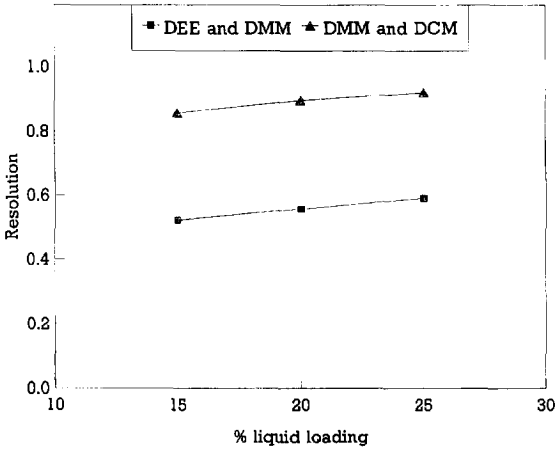

Fig. 7. Effect of percentage liquid loading on resolution in desorption section. $L = 1.0$ m, $L' = 2.0$ m, $u_0 = 0.15$ m/s, 35°C, 45–60 mesh.

section. However, the mathematical model of the uniform film thickness concept might be used for a simple estimation of the optimum operating conditions for a combined continuous and preparative chromatographic system.

5. Conclusions

Mathematical models have been adopted to simulate the performance of a combined continuous and preparative chromatographic system. The model equations were the transient material balances with the assumption of a uniform film thickness of SLP on a porous solid support and linearity of the equilibrium isotherm, and these were used to investigate the number of theoretical plates and the resolution of the DEE, DMM and DCM with various operating conditions.

Among the various conditions, an additional column length in the desorption section greatly influenced the resolution of the components. Continuous operation could be achieved if the feed materials of ternary mixture were separated by adjusting the additional column length and the desorbent velocity in the desorption section within the switching time.

Symbols

a_i	peak width of component i cut by the two tangents in unit volume, m^3
A_p	surface area of porous particle per unit volume, m^2/m^3
b_i	retention volume of component i from injection to peak maximum, m^3
c	concentration of solute in the mobile phase, mol/m^3
c_0	inlet concentration of solute, mol/m^3
$C(s)$	Laplace transform of $c(t)$
D_e	effective diffusion coefficient, m^2/s
D_l	diffusion coefficient in SLP, m^2/s
D_M	molecular diffusion coefficient, m^2/s
DEE	diethyl ether
DMM	dimethoxymethane
DCM	dichloromethane
E	axial dispersion coefficient, m^2/s
k_f	interparticle mass transfer coefficient, m/s
k_g	intraparticle mass transfer coefficient with respect to SLP film, m/s
K	partition coefficient
L	column length in the partition section and desorption section, m
L'	additional column length in the desorption section, m
N	number of theoretical plates calculated by Eq. 18
r_p	radius of spherical porous particle, m
R	resolution defined by Eq. 19
Re	particle Reynolds number
s	variable of Laplace transform with respect to time
Sc	Schmidt number
SLP	stationary liquid phase
t	time, s
t_0	time of feed injection, s
u	interstitial velocity of carrier gas or desorbent, m/s
u_0	superficial velocity of carrier gas or desorbent, m/s
$v_{1/2}$	retention volume corresponding to half-height, m^3
w	intercept under the tangent at the point of inflection in units of volume, m^3
z	axial distance, m

Greek letters

γ, γ_1–γ_5	values defined by Eqs. 10–15
δ	film thickness of stationary liquid phase, m
ϵ	interparticle void fraction of chromatographic column
ϵ_p	intraparticle void fraction in presence of SLP
λ, λ_1–λ_3	values defined by Eqs. 2–5

References

[1] C.J. King, Separation Processes, McGraw-Hill, New York, 2nd ed., 1980.

[2] D.H. James and C.S.G. Phillips, J. Chem. Soc., (1953) 1600.
[3] E. Grushka (Editor), Preparative Scale Chromatography, Marcel Dekker, New York, 1989.
[4] G. Subramanian (Editor), Preparative and Process-Scale Liquid Chromatography, Ellis Horwood, New York, 1991.
[5] P.E. Barker and D. Critcher, Chem. Eng. Sci., 13 (1960) 82.
[6] G.R. Fitch, M.E. Probert and P.F. Tiely, J. Chem. Soc., (1960) 4892.
[7] P.E. Barker, in C.H. Knapman (Editor), Developments in Chromatography, Applied Science, London, 1978.
[8] B.B. Fish, R.W. Carr and R. Aris, AIChE J., 35 (1989) 737.
[9] D.B. Broughton, Chem. Eng. Prog., 64 (1969) 60.
[10] K. Hashimoto, S. Adachi, H. Noujima and A. Maruyama, J. Chem. Eng. Jpn., 16 (1983) 400.
[11] K. Hashimoto, S. Adachi, H. Noujima and Y. Udea, Biotechnol. Bioeng., 25 (1983) 2371.
[12] P.E. Barker, K. England and G. Vlachogiannis, Chem. Eng. Res. Des., 61 (1983) 241.
[13] C.B. Ching and D.M. Ruthven, Chem. Eng. Sci., 40 (1985) 877.
[14] C.B. Ching and D.M. Ruthven, Chem. Eng. Sci., 40 (1985) 1411.
[15] B.B. Fish, R.W. Carr and R. Aris, AIChE J., 39 (1993) 1783.
[16] C.B. Ching, K.H. Chu and K. Hidajat, AIChE J., 40 (1994) 1843.
[17] G. Storti, R. Baciocchi, M. Mazzotti and M. Morbidelli, Ind. Eng. Chem. Res., 34 (1995) 288.
[18] P.C. Wankat, Ind. Eng. Chem. Fundam., 16 (1977) 468.
[19] P.C. Wankat, Ind. Eng. Chem. Fundam., 23 (1984) 256.
[20] H.Y. Ha, K.H. Row and W.K. Lee, Sep. Sci. Technol., 22 (1987) 141.
[21] K.H. Row, presented at the 11th International Symposium on Preparative and Industrial Chromatography, Baden-Baden, 3–5 October 1994.
[22] K.H. Row and W.K. Lee, in N.P. Cheremisinoff (Editor), Separation by Gas–Liquid Chromatography (Handbook of Heat and Mass Transfer, Vol. 3: Catalysis, Kinetics, and Reactor Engineering), Gulf, Houston, TX, 1989, Ch. 22.
[23] K.H. Row and W.K. Lee, J. Chem. Eng. Jpn., 19 (1986) 173.
[24] M.A. Alkarasani and B.J. McCoy, Chem. Eng. J., 23 (1982) 81.
[25] N.D.P. Dang and L.G. Gibilaro, Chem. Eng. J., 8 (1974) 157.
[26] S.C. Foo and R.G. Rice, AIChE J., 21 (1975) 16.
[27] S.Ergun, Chem. Eng. Prog., 48 (1952) 227.
[28] A.B. Seid, Theory and Mathematics of Chromatography, Schwetzinger Verlagsdruckerei, Schwetzingen, 1981.
[29] L. Personaz and P. Gareil, Sep. Sci. Technol., 16 (1981) 13.
[30] P. Valentin and G. Guiochon, Sep. Sci. Technol., 10 (1975) 289.